THE JOURNAL OF BIOLOGICAL CHEMISTRY VOL. 286, NO. 16, pp. 14120–14128, April 22, 2011

Kir4.1 Channel Expression Is Essential for Parietal Cell Control of Acid Secretion*

Received for publication, June 4, 2010, and in revised form, January 20, 2011 Published, JBC Papers in Press, March 2, 2011, DOI 10.1074/jbc.M110.151191

Penghong Song[‡1], Stephanie Groos[§], Brigitte Riederer[‡], Zhe Feng[‡], Anja Krabbenhöft[‡], Michael P. Manns[‡], Adam Smolka[¶], Susan J. Hagen[‖], Clemens Neusch[**], and Ursula Seidler[‡2]

From the Departments of [‡]Gastroenterology, Hepatology, and Endocrinology and [§]Anatomy I, Hannover Medical School, D-30625 Hannover, Germany, the [¶]Department of Medicine, Medical University of South Carolina, Charleston, South Carolina 29403, the [‖]Department of Surgery, Beth Israel Deaconess Medical Center, Boston, Massachusetts 02115, and the [**]Department of Neurology, University of Göttingen, D-37075 Göttingen, Germany

Kir4.1 channels were found to colocalize with the H^+/K^+-ATPase throughout the parietal cell (PC) acid secretory cycle. This study was undertaken to explore their functional role. Acid secretory rates, electrophysiological parameters, PC ultrastructure, and gene and protein expression were determined in gastric mucosae of 7–8-day-old Kir4.1-deficient mice and WT littermates. Kir4.1$^{-/-}$ mucosa secreted significantly more acid and initiated secretion significantly faster than WT mucosa. No change in PC number but a relative up-regulation of H^+/K^+-ATPase gene and protein expression (but not of other PC ion transporters) was observed. Electron microscopy revealed fully fused canalicular membranes and a lack of tubulovesicles in resting state Kir4.1$^{-/-}$ PCs, suggesting that Kir4.1 ablation may also interfere with tubulovesicle endocytosis. The role of this inward rectifier in the PC apical membrane may therefore be to balance between K^+ loss via KCNQ1/KCNE2 and K^+ reabsorption by the slow turnover of the H^+/K^+-ATPase, with consequences for K^+ reabsorption, inhibition of acid secretion, and membrane recycling. Our results demonstrate that Kir4.1 channels are involved in the control of acid secretion and suggest that they may also affect secretory membrane recycling.

The regulation of gastric acid secretion requires the coordinated function of a variety of parietal cell (PC)[3] apical and basolateral ion transport pathways, as well as the fusion of H^+/K^+-ATPase-containing tubulovesicles with the resting state apical membrane and their endocytosis after withdrawal of the secretory stimulus (1–3). Several molecules have been recently identified that are involved in the exo/endocytotic machinery of the PC apical membrane (4). However, it is unclear how the ionic requirements, which have proven essential for endocytosis in other cells (5), may be met at the extracellular face of the PC secretory membrane at the end of the secretory cycle.

The PC expresses two types of K^+ channels in the apical membrane (6, 7). KCNQ1 and its subunit KCNE2 are highly expressed in PCs (8, 9), and recent work by several groups has unequivocally confirmed the concept that KCNQ1/KCNE2 channels are the K^+ channels that provide K^+ to the external binding site of the H^+/K^+-ATPase of the PC secretory membrane during acid secretion (10, 11).

However, Fujita *et al.* (12) found several members of the Kir family of inwardly rectifying K^+ channels expressed in rat gastric mucosa, and this was confirmed by others (9, 13, 14). The only study in which PC tubulovesicular and secretory membranes were isolated, reconstituted in lipid bilayer, and studied electrophysiologically found channels with Kir rather than KCNQ1 channel properties (13). Furthermore, a recent study demonstrated co-precipitation of H^+/K^+-ATPase and Kir4.1 from both immunopurified tubulovesicles and stimulated secretory membranes, as well as a complete translocation of not only H^+/K^+-ATPase but also of Kir4.1 from the tubulovesicular to secretory membrane pool (14), but the physiological role of these channels remained unexplained. We therefore searched for an experimental model to elucidate the physiological role of the PC Kir4.1 channels. Because Kir4.1-deficient mice develop early neurological deficits and die soon after birth, we investigated the acid secretory capacity, PC ultrastructure, and gene expression of isolated gastric mucosae from 7–8-day-old Kir4.1-deficient, WT, and heterozygous mice.

MATERIALS AND METHODS

Animals—Kir4.1$^{+/+}$ and Kir4.1$^{-/-}$ mice were originally generated in the laboratory of Henry A. Lester (15) and raised on the original 129/SVJ background in the animal facility of Hannover Medical School or the University of Göttingen. All studies were approved by the Committee on Investigations Involving Animals, Hannover Medical School, and the University of Göttingen and by an independent review committee composed by the State Government Agency for animal welfare. All mice were 7–8 days of age. The genotypes of the mice were verified by PCR.

Measurement of Acid Secretory Rates in Isolated Gastric Mucosa—The experiments were performed as described previously (43) with the modifications indicated below. After killing

* This work was supported by Deutsche Forschungsgemeinschaft Sachbeihilfe Se460/9-5 and Se460/9-6 and by the Lower Saxony Ministry of Science and Education and the Volkswagen Vorab Stiftung (to U. S.).

[1] Present address: Key Laboratory of Combined Multiorgan Transplantation, Ministry of Public Health, The First Affiliated Hospital, School of Medicine, Zhejiang University, Hangzhou 310003, China.

[2] To whom correspondence should be addressed: Dept. of Gastroenterology, Hepatology, and Endocrinology, Hannover Medical School, Carl-Neuberg-Str. 1, D-30625 Hannover, Germany. Tel.: 49-511-532-9427; Fax: 49-511-532-8428; E-mail: seidler.ursula@mh-hannover.de.

[3] The abbreviations used are: PC, parietal cell; PD, potential difference; KO, knock-out; BisTris, 2-[bis(2-hydroxyethyl)amino]-2-(hydroxymethyl)-propane-1,3-diol.

the animals by cervical dislocation, the stomach was cleaned in ice-cold Ringer's solution (145.5 mM NaCl, 4 mM KCl, 1.2 mM $CaCl_2$, and 0.05 mM indomethacin) and mounted between two Lucite half-chambers (with an exposed surface area of 0.283 cm^2) of a water-jacketed Ussing system equipped with a gas-lift system. The serosal solution contained 108 mM NaCl, 22 mM $NaHCO_3$, 3 mM KCl, 1.3 mM $MgSO_4$, 2 mM $CaCl_2$, 2.25 mM KH_2PO_4, 8.9 mM glucose, 10 mM sodium pyruvate, 3×10^{-2} mM indomethacin, and 10^{-3} mM tetrodotoxin to minimize variation due to intrinsic prostanoids and neural tone and was gassed with 95% O_2 and 5% CO_2 (pH 7.4). The mucosal solution contained 154 mM NaCl and was gassed with 100% O_2 and kept at constant pH 7.4 with 2 mM NaOH by a pH-stat titration system (Radiometer, Copenhagen, Denmark). The volume of the titrant infused per unit time was used to quantify H^+ secretion. These measurements were recorded at 5-min intervals. The rate of luminal H^+ secretion (J_{H^+}) is expressed as $\mu mol \cdot cm^{-2} \cdot h^{-1}$. Transepithelial short-circuit current (I_{sc}; reported as $\mu eq \cdot cm^{-2} \cdot h^{-1}$) and potential difference (PD; expressed as mV) were measured via an automatic voltage clamp (EVC-4000 voltage-current clamp, World Precision Instruments, Berlin, Germany). Transepithelial resistance (R_t; reported as ohms·cm^2) was calculated according to values of I_{sc} and PD. Basal parameters were measured for a period of 30 min if the stomach showed spontaneous acid secretion, and then stimulant (10^{-5} M forskolin) was added to the serosal side of the tissue. Changes in gastric acid secretion, I_{sc}, R_t, and PD were determined during the 60 min after the addition of stimulants.

Only stomachs that secreted acid after forskolin stimulation and displayed normal electrophysiological parameters and no signs of leakage (rapid increase in luminal pH, indicative of an HCO_3^- leak from the serosal perfusate) were included in calculations of the time course and magnitude of stimulation of acid secretion by forskolin. Equal numbers of WT, heterozygous, and knock-out (KO) mucosae were excluded because of leakiness or lack of PD buildup. In a subset of experiments, the luminal perfusate was 154 mM KCl.

Light and Transmission Electron Microscopy—The stomachs were removed and immediately immersed in a fixative solution containing either 2% glutaraldehyde and 2% formaldehyde (freshly prepared from paraformaldehyde) buffered in 0.1 M sodium cacodylate/HCl buffer (pH 7.3) or 4% formaldehyde (freshly prepared from paraformaldehyde) in the same buffer. The stomachs were opened along the limiting ridge separating the keratinized forestomach from the glandular stomach. To ascertain the presence of comparable segments in all specimens, small fragments (1–2 mm) from the gastric fundus were prepared with the same distance from this limiting ridge. The fragments were transferred into fresh fixative solution and stored for at least 4 h at 4 °C. For light and transmission electron microscopy, specimens fixed in the presence of glutaraldehyde were washed with 0.1 M sodium cacodylate/HCl (pH 7.3), post-fixed for 90 min in 2% OsO_4 buffered in 0.1 M sodium cacodylate/HCl (pH 7.3), and subsequently dehydrated in increasing concentrations of ethanol and finally embedded in epoxy resin (Serva, Heidelberg, Germany). Thick plastic sections (1 μm) were prepared with a Reichert Ultracut E ultramicrotome (Leica, Wetzlar, Germany), stained with alkalinized toluidine blue, and observed with a Leitz Orthoplan light microscope (Leica) equipped with a CCD camera (Olympus DP50). Thin sections were collected on Formvar-coated copper slot grids, stained with uranyl acetate and lead citrate, and examined using a Zeiss EM 10 CR transmission electron microscope at an acceleration voltage of 80 kV.

Immunofluorescence—Formaldehyde-fixed specimens were dehydrated and embedded as described above but without post-fixation. Semithin sections (1 μm) of these samples were collected on glass slides pretreated with 3-(triethoxysilyl)propylamide (silane; Merck, Darmstadt, Germany). The sections were etched for 20 min in sodium ethoxide diluted to 50% with absolute ethanol. After washing with PBS, nonspecific protein binding was blocked with the application of 5% BSA diluted in PBS for 30 min at room temperature. Incubation with mouse anti-H^+/K^+-ATPase monoclonal antibody (HK 12.18) diluted 1:2500 in PBS with the addition of 1% BSA was performed overnight at 4 °C in a humid chamber. After thorough rinsing in PBS, the sections were incubated for 60 min at room temperature with goat anti-mouse IgG conjugated to Alexa 488 (Molecular Probes, Eugene, OR). Laser scanning confocal microscopy was performed using a Zeiss Axiovert 200 M microscope attached to an LSM 510 META detector controlled by LSM 5 Image Version 3.2 software (Zeiss).

Morphometric Analysis—Parietal cells were counted on toluidine blue-stained semithin sections of stomach specimens (three mice per group) using a Leitz Orthoplan light microscope with a ×40 objective lens. Only glands that were sectioned perpendicular to their length axis were evaluated. For better visualization and quantification of tubulovesicular structures and secretory membranes in the electron micrographs, we asked an expert histologist to outline the tubulovesicles in blue and the secretory membranes with apical microvilli in red. We adapted this method from Ref. 17. Further quantification was not performed.

Quantitative Real-time PCR—RNA isolation was performed from the glandular stomach epithelia (fundus and corpus) of 7-day-old Kir4.1-deficient mice and their WT littermates, and quantitative RT-PCR was performed as described by Song *et al.* (11). In addition, the mRNA expression of KCNQ1 was investigated. Primer sequences were as follows: KCNQ1, 5′-GGAACATAGGGATGGGGAGT-3′ (forward) and 5′-GTTCCCTGATGGTCTCTG GA-3′ (reverse). The PCR product length was 151 bp (potassium voltage-gated channel, subfamily Q, member 1, Mouse Genome Database ID NM_008434).

Western Analysis of the H^+/K^+-ATPase α-Subunit—Gastric mucosae from 7-day-old Kir4.1-deficient mice and their WT littermates were homogenized with Ultra-Turrax in PBS containing 1 mM EGTA, 1% Triton X-100, 0,1% SDS, 20 μg/ml antipain, 4 mM benzamidine, 1 mM DTT, 20 μg/ml leupeptin, 20 μg/ml pepstatin A, and 40 μg/ml PMSF. After centrifugation at 12,000 × *g* for 2 min at 4 °C, the supernatant was aliquoted and stored at −80 °C. 10 μg of homogenate was size-fractionated on 10% NuPAGE Novex BisTris gels (Invitrogen) under denaturing conditions, transferred to PVDF membranes (Hybond-P, GE Healthcare, Little Chalfont, United Kingdom), and blocked with 5% nonfat dry milk in Tris-buffered saline/Tween. Blots were probed at 4 °C with mouse anti-H^+/K^+-

TABLE 1

Body weights of 7-day-old Kir4.1$^{+/+}$, Kir4.1$^{+/-}$, and Kir4.1$^{-/-}$ pups

The body weights of Kir4.1$^{-/-}$ mice on day 7 were significantly reduced compared with their Kir4.1$^{+/+}$ and Kir4.1$^{+/-}$ littermates ($p < 0.001$). Null mutants exhibited little growth beyond that age, with few exceeding 4 g.

Genotype	Weight
	g
Kir4.1$^{+/+}$ ($n = 23$)	4.88 ± 0.17
Kir4.1$^{+/-}$ ($n = 17$)	4.87 ± 0.19
Kir4.1$^{-/-}$ ($n = 19$)	3.46 ± 0.08

ATPase β-subunit monoclonal antibody (clone 2G11, Sigma), diluted 1:4000 and with rabbit anti-β-actin polyclonal antibody (1:15,000; ab8227, Abcam, Cambridge, United Kingdom). The secondary antibodies were goat anti-mouse and goat anti-rabbit IgG conjugated to horseradish peroxidase (KPL, Gaithersburg, MD), both diluted 1:10,000 in Tris-buffered saline/Tween, and incubated for 1 h at room temperature. The antigen-antibody complexes on the PVDF membranes were visualized by chemiluminescence (ECL Western blotting detection reagents, GE Healthcare), and the image was captured on light-sensitive imaging film (Hyperfilm ECL, GE Healthcare). Bands were detected and digitized by the BioDocAnalyze image station (Biometra, Göttingen, Germany), and the optical density was measured using TotalLab software (Nonlinear Dynamics, Durham, United Kingdom). The ratio H^+/K^+-ATPase of β-actin was calculated from individual lanes, each representing protein from one single Kir4.1 mouse.

Statistics—All results are expressed as means ± S.E. ΔJ_{H^+} refers to stimulated peak responses minus basal levels. Basal values for J_{H^+}, I_{sc}, and R_t refer to an average taken over a 30-min base-line period. Data were analyzed by Student's *t* tests or by one-way analysis of variance with the Student-Newman-Keuls post hoc test. A *p* value of <0.05 was considered statistically significant.

RESULTS

Body Weights of Kir4.1 KO, Heterozygous, and WT Mice—Genotype frequencies of Kir4.1 in pups from heterozygous matings exhibited a normal Mendelian ratio of 1:2:1 with no alteration in the percentage of male or female null mutant mice. Kir4.1$^{-/-}$ mice were indistinguishable at birth from their WT littermates but developed progressive growth failure after ~4–5 days (Table 1), displaying a mortality rate of 100% at day 14. In addition, they developed motor coordination deficits at ~1 week after birth (18). We used pups that were 7–8 days of age, at which age both WT and mutant mice had stable basal as well as forskolin-stimulated acid secretory rates that were about one-fourth of those seen in adult mice. Only mice that had milk in the stomach after being killed were used for the experiments because this indicated normal suckling behavior in WT and mutant mice. Most litters contained one to two Kir4.1$^{-/-}$ mice at birth, but most Kir4.1$^{-/-}$ mutants died before day 7. When we genotyped at days 1–2 after birth and reduced litter size by removing some Kir4.1$^{+/+}$ and Kir4.1$^{+/-}$ mice, then the Kir4.1$^{-/-}$ mice had higher weights and longer survival.

Effect of Forskolin on Gastric Acid Secretion in Kir4.1 KO, Heterozygous, and WT Mice—Spontaneous acid secretion was observed at low and not significantly different rates in Kir4.1$^{+/+}$, Kir4.1$^{+/-}$, and Kir4.1$^{-/-}$ gastric mucosae. The addition of 10^{-5} M forskolin resulted in a strong stimulation of acid secretion in all genotypes. Surprisingly, in the first 10 min after forskolin stimulation, the acid secretory rate increased more than twice as fast in Kir4.1$^{-/-}$ mucosa than in Kir4.1$^{+/+}$ or Kir4.1$^{+/-}$ mucosa (Fig. 1, *A* and *B*), with a marked overshoot. At 30 min post-forskolin, the acid secretory rates between Kir4.1$^{+/+}$ and Kir4.1$^{-/-}$ mucosae had become similar, but the total acid output during the experiment was significantly higher in Kir4.1$^{-/-}$ mucosa (Fig. 1*C*). No significant differences were observed in the PD, I_{sc}, and R_t of Kir4.1$^{+/+}$, Kir4.1$^{+/-}$, and

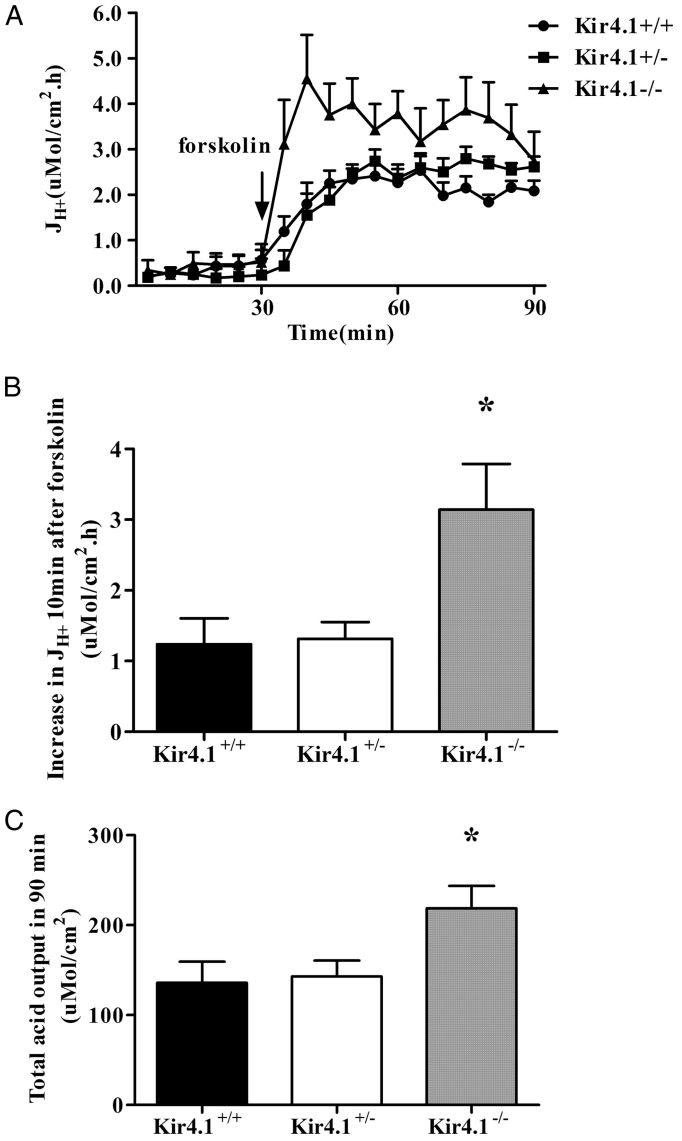

FIGURE 1. **Effects of forskolin (10^{-5} M) on gastric acid secretion in the presence and absence of Kir4.1 expression.** *A*, time course of acid secretory rates (J_{H^+}) in the basal state and in response to forskolin added to the serosal bath at 30 min after the start of measuring the basal secretory rate. *B*, increase in J_{H^+} in the first 10 min after the addition of forskolin. *C*, the total acid output in 90 min was calculated as the area under the curve. Forskolin-stimulated increase in J_{H^+} after 10 min was significantly faster in Kir4.1$^{-/-}$ mucosa compared with Kir4.1$^{+/+}$ or Kir4.1$^{+/-}$ mucosa. Also, total acid output over the whole experiment was significantly higher in Kir4.1$^{-/-}$ mucosa compared with WT or Kir4.1$^{+/-}$ mucosa but less strong than the increase in J_{H^+} in the first 10 min after stimulation. *, $p < 0.05$. $n = 14$ for Kir4.1$^{+/+}$, $n = 18$ for Kir4.1$^{+/-}$, and $n = 8$ for Kir4.1$^{-/-}$. Values are expressed as means ± S.E.

TABLE 2

Electrical parameters for acid secretion experiments

Shown are the effects of forskolin (10^{-5} M) on the PD, I_{sc}, and R_t of gastric mucosae from Kir4.1$^{+/+}$, Kir4.1$^{+/-}$, and Kir4.1$^{-/-}$ mice before and 30 min after forskolin stimulation. No significant difference in PD, I_{sc}, and R_t was observed at these time points in Kir4.1$^{+/+}$, Kir4.1$^{+/-}$, and Kir4.1$^{-/-}$ mice ($p < 0.05$). The values were calculated from six out of eight experiments with Kir4.1$^{-/-}$ mucosa and a matched Kir4.1$^{+/+}$ and Kir$^{+/-}$ mucosa for each Kir$^{-/-}$ mucosa. Values are expressed as means ± S.E.

	PD		I_{sc}		R_t	
	Basal	30 min post-forskolin	Basal	30 min post-forskolin	Basal	30 min post-forskolin
	mV		$\mu eq \cdot cm^{-2} \cdot h^{-1}$		$\omega \cdot cm^2$	
Kir4.1$^{+/+}$ ($n = 6$)	22.59 ± 1.25	26.28 ± 1.69	10.40 ± 1.00	12.28 ± 1.37	98.28 ± 5.89	82.40 ± 7.39
Kir4.1$^{+/-}$ ($n = 6$)	23.39 ± 1.67	27.08 ± 2.19	10.62 ± 1.05	13.70 ± 1.80	100.40 ± 7.35	94.31 ± 6.70
Kir4.1$^{-/-}$ ($n = 6$)	21.39 ± 1.65	26.41 ± 2.40	8.83 ± 0.91	11.56 ± 1.21	106.07 ± 5.00	94.84 ± 5.13

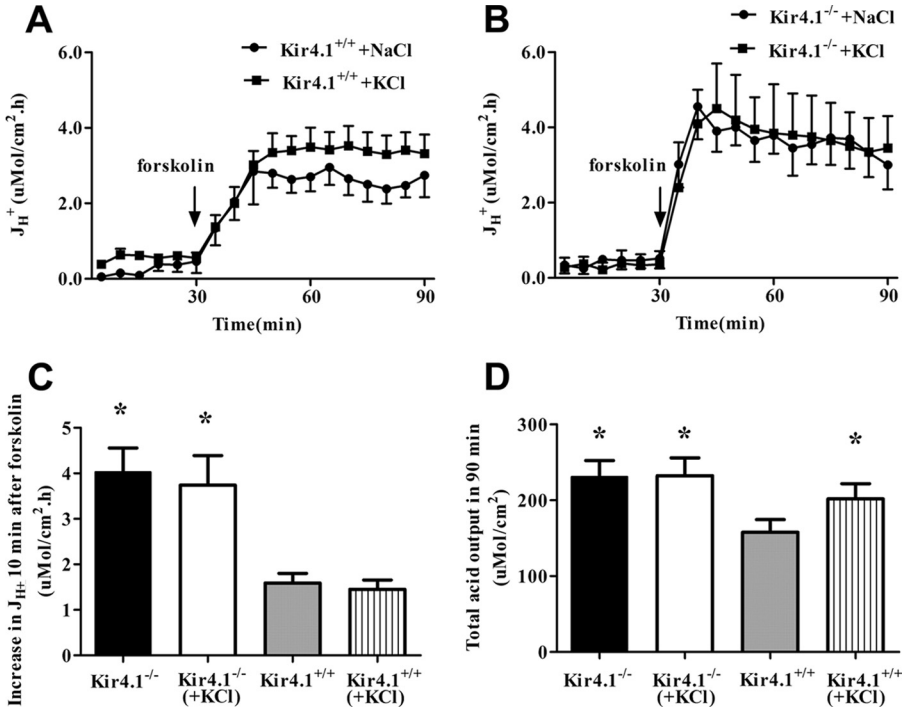

FIGURE 2. **Effect of forskolin (10^{-5} M) on gastric acid secretion in the presence of 154 mM luminal NaCl or KCl.** *A* and *B*, time courses of acid secretory rate (J_{H^+}) in the basal state and in response to forskolin added to the serosal bath at 30 min after the start of measuring the basal secretory rate in 154 mM KCl or NaCl in the luminal bath in Kir4.1$^{+/+}$ or Kir4.1$^{-/-}$ mucosa, respectively. *C*, the forskolin-stimulated increase in J_{H^+} after 10 min was not significantly increased in Kir4.1$^{-/-}$ or Kir4.1$^{+/+}$ mucosa in the presence of high luminal K^+. *D*, however, the steady-state J_{H^+} after forskolin addition and total acid output during the 90 min were significantly increased in the presence of luminal KCl compared with NaCl in Kir4.1$^{+/+}$ mucosa, but not Kir4.1$^{-/-}$ mucosa. *, $p < 0.05$. $n = 7$ for Kir4.1$^{+/+}$ in KCl, $n = 8$ for Kir4.1$^{+/+}$ in NaCl, $n = 4$ for Kir4.1$^{-/-}$ in KCl, and $n = 6$ for Kir4.1$^{-/-}$ in NaCl. Values are expressed as means ± S.E.

Kir4.1$^{-/-}$ mucosae basally and when the maximal secretory rate had been reached in all genotypes (30 min after stimulation) (Table 2).

Effect of Forskolin on Acid Secretory Rates in the Presence of High Luminal K^+ in Kir4.1 WT and KO Mice—In the next set of experiments, acid secretion was measured in the presence of either a high luminal K^+ concentration (154 mM KCl) or saline (154 mM NaCl). After 30 min in the respective luminal solution, the tissues were stimulated with forskolin. In WT mucosa, the presence of high luminal K^+ resulted in a significant increase in overall acid output (Fig. 2*D*), but not in a more rapid onset of acid secretion (Fig. 2*C*). This indicates that luminal K^+ is a rate-limiting factor for acid secretory rate in isolated mucosa of 7-day-old WT mice but does not accelerate the speed of onset of secretion. In Kir4.1$^{-/-}$ mucosa, no significant differences were found between high luminal K^+ and saline (Fig. 2, *C* and *D*). These results suggest that high luminal K^+ can mimic high total acid secretory outputs seen in Kir4.1$^{-/-}$ mucosa, but not the rapid onset of acid secretion, the reasons for which must be sought elsewhere. We therefore studied Kir4.1$^{-/-}$ gastric mucosa and its PCs morphologically.

Histological, Immunohistochemical, and Electron Microscopic Evaluation of Kir4.1 KO and WT Gastric Mucosae—The oxyntic mucosal epithelium of 7–8-day-old mice was routinely composed of numerous mucous neck cells, surface cells, chief cells, endocrine cells, and distinctive PCs, which were found along the gland, including the gland base (Fig. 3*A*), No significant differences in PC number between the WT and Kir4.1-deficient mucosae were observed (Fig. 3*B*). Laser scanning confocal microscopy of gastric gland sections labeled with antibody against gastric H^+/K^+-ATPase revealed similar localization of this enzyme in Kir4.1-deficient mice and WT littermates. In suitable section planes, H^+/K^+-ATPase was routinely observed bordering the apical plasma membrane (Fig. 3*C*).

PC morphology was further studied by electron microscopy. WT PCs showed intracellular canaliculi lined with numerous microvilli. Close to the canaliculi, membranes of the tubulovesicular system were visible in resting state mucosa (Fig. 4, *A* and

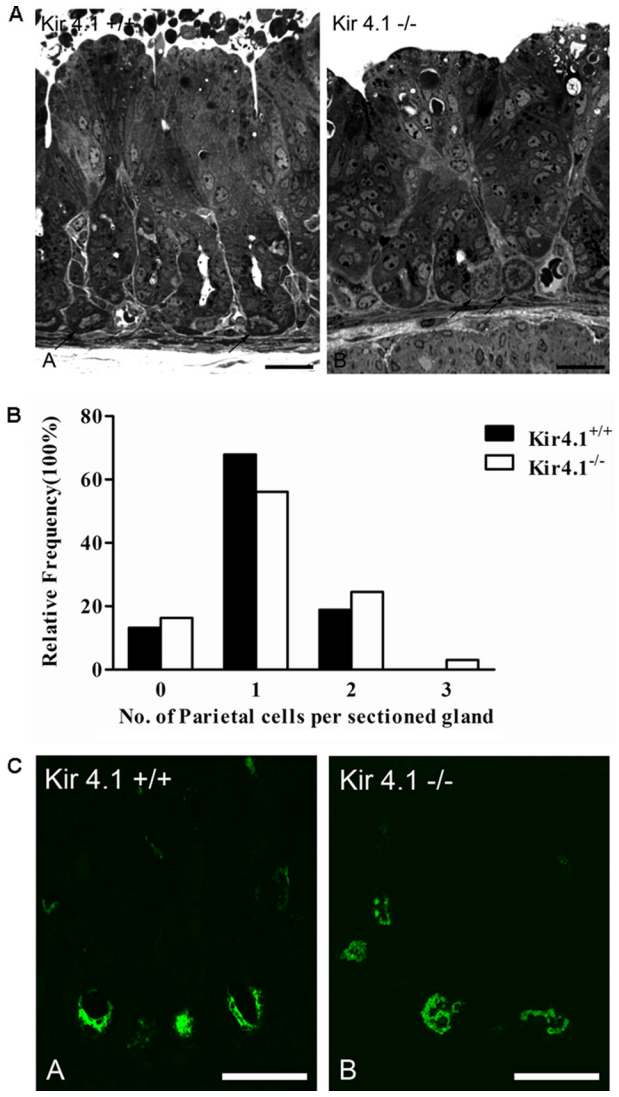

FIGURE 3. *A*, light microscopy of semithin sections of Kir4.1$^{+/+}$ and Kir4.1$^{-/-}$ stomach mucosae. In both genotypes, droplets of varying size can be observed in the cells directly lining the lumen, indicative of milk absorption. Some of the PCs in the young mice were also found at the base of the glands. *B*, relative frequency distribution of the number of PCs in sections of gastric glands did not differ between Kir4.1$^{+/+}$ and Kir4.1$^{-/-}$ mice (a total of three pairs was analyzed). *C*, confocal images of semithin sections of WT and KO gastric mucosae labeled with mouse monoclonal antibody against H^+/K^+-ATPase. No obvious difference in the fluorescence intensity between the +/+ and −/− genotypes was seen. *Scale bars* = 25 μm. Five total pairs of Kir4.1$^{-/-}$ and WT stomachs were analyzed.

B). Occasional PCs that showed the morphologic features of spontaneous secretion were also identified in WT gastric mucosa (Fig. 4, *C* and *D*).

The ultrastructural morphology of the Kir4.1-deficient PCs appeared different from that of the WT littermates (Fig. 5, *A–D*). The conspicuous difference was that in the resting state PCs from Kir4.1 KO mice, the microvilli (labeled in *red* in the large magnifications) of the secretory canaliculi were much more elaborate than those in resting state WT PCs, even though the lumina of the canaliculi were not expanded (Fig. 5, *A–D*). In addition, tubulovesicular structures (labeled in *blue* in the large magnifications) near the canaliculi, as seen in the WT PCs, were absent or rare. In summary, Kir4.1-deficient cells displayed fused secretory membranes as fully stimulated cells do but without expansion of the intracanalicular spaces (consistent with the low acid secretory rates found for these unstimulated mucosae) (Fig. 1). For better visualization of the observed differences, tubulovesicular structures are outlined in *blue* and secretory canaliculi in *red* in the higher magnification images of all electron micrographs shown.

H^+/K^+-ATPase, KCNQ1, Kir5.1, and AE2 mRNA Expression in Kir4.1 KO and WT Gastric Mucosae—mRNA levels for a number of PC-specific or PC-enriched genes were determined. The results were striking: although H^+/K^+-ATPase mRNA expression was significantly increased, the expression levels for the apical K^+ recycling channels KCNQ1, Kir5.1 (the likely partner for Kir4.1), and basolateral anion exchanger AE2 were not significantly different in Kir4.1-deficient and WT mucosae (Fig. 6).

Western Analysis of H^+/K^+-ATPase Protein in Gastric Mucosal Homogenates of Kir4.1 KO and WT Mice—The increase in H^+/K^+-ATPase mRNA expression could reflect instability of the apical membrane with increased H^+/K^+-ATPase turnover. We therefore investigated whether it was paralleled by an increase in H^+/K^+-ATPase protein. We performed Western analysis of total fundus/corpus mucosal protein lysates. At day 7, a Kir4.1$^{-/-}$ sibling was present in only ~30% of the litters. We were able to analyze a total of four litters, which contained one Kir4.1$^{-/-}$ sibling, one to three Kir4.1$^{+/+}$ siblings, and various numbers of Kir4.1$^{+/-}$ siblings, which were not included in the analysis. We found a significant increase in the H^+/K^+-ATPase α-subunit in Kir4.1$^{-/-}$ mucosa (Fig. 7, *A* and *B*). This may explain in part the increase in 1-h acid output in the Kir4.1$^{-/-}$ stomachs compared with WT stomachs, whereas the increase in speed of onset of secretion may be explained by the difference in secretory membrane architecture between Kir4.1$^{-/-}$ and WT PCs.

DISCUSSION

The data in this study show that the loss of Kir4.1 channels results in marked changes in the acid secretory pattern in isolated gastric mucosae of young mice, with an up-regulation of H^+/K^+-ATPase mRNA and protein expression and an exaggerated H^+ secretory response to acid secretagogs. In addition, a different ratio of tubulovesicular to secretory membrane structures in the resting state PC was observed, which may point to a defect in tubulovesicle endocytosis.

How can the observed changes be reconciled with the absence of an inwardly rectifying K^+ channel in PC tubulovesicles and secretory membranes? When colocalization of Kir4.1 with the H^+/K^+-ATPase in the tubulovesicles as well as the stimulated secretory membranes had been observed (12–14), we and others believed that Kir4.1 channels may serve to bring K^+ to the extracellular K^+-binding site of the H^+/K^+-ATPase during stimulation of acid secretion. In this scenario, the acid secretory rate should be decreased in Kir4.1 KO mucosa.

Surprisingly, the lack of Kir4.1 resulted not in a diminished but in a higher acid secretory rate than in WT mucosa. Because increasing the luminal K^+ concentration to supraphysiological values also augmented the acid secretory range in WT mucosa (Fig. 2), but not in Kir4.1$^{-/-}$ mucosa, the role of this inwardly

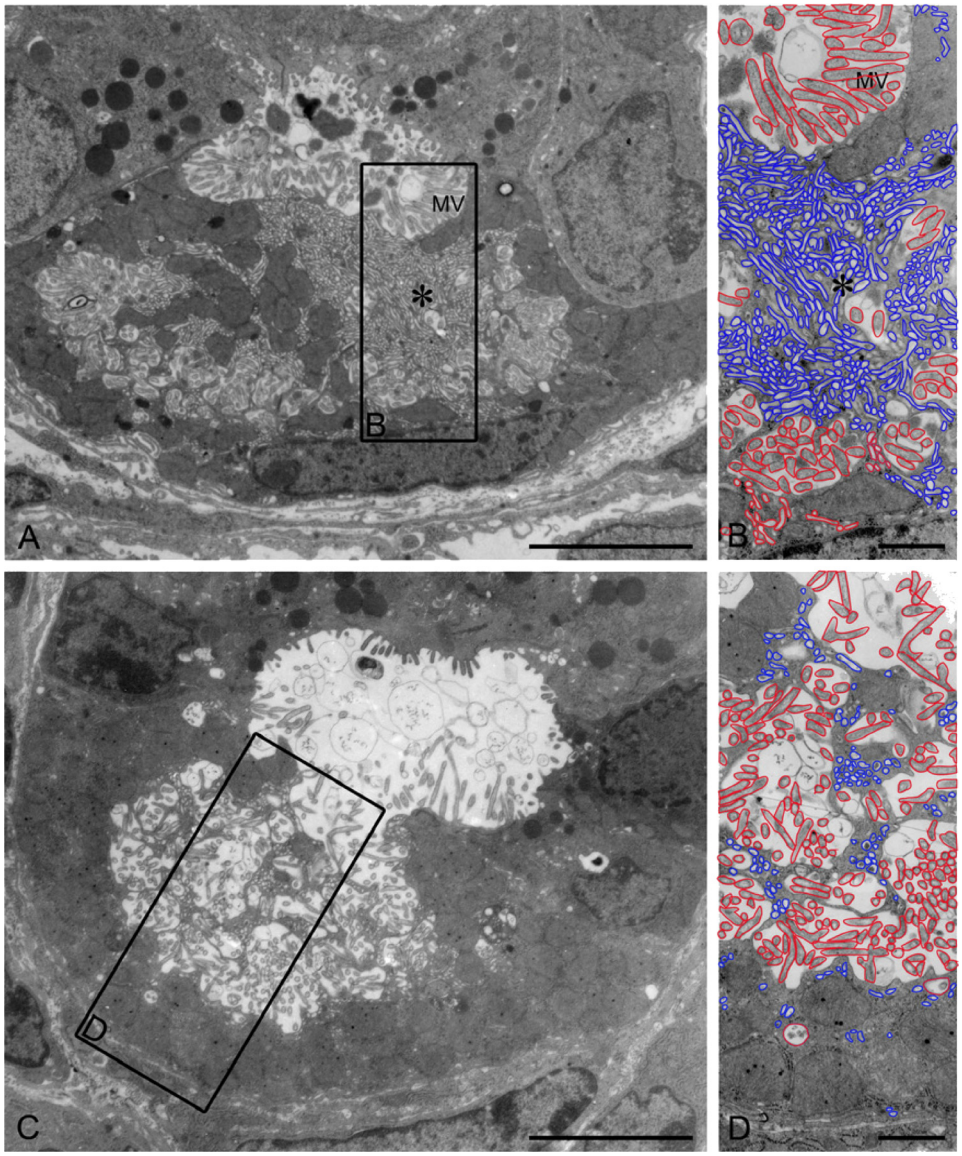

FIGURE 4. **Transmission electron microscopy of stomach mucosa from unstimulated WT oxyntic cells, with some cells more in the resting state (*A* and *B*) and some cells in a spontaneously secreting state (*C* and *D*).** In the resting state, numerous tubulovesicular (tubulocisternal) structures are seen (enlarged in *B* and *D*). *Scale bars* = 5 μm (*A* and *C*) and 1 μm (*B* and *D*). For better visualization, all tubulocisternal structures are delineated in *blue*, and all microvillus (*MV*)-containing secretory membranes are outlined in *red*.

rectifying K^+ channel may be to provide the balance between rapid K^+ loss via KCNQ1/KCNE2 and slower K^+ reabsorption by the slow turnover of the H^+/K^+-ATPase. An electrochemical gradient for such an action may be present in the stimulated secretory membranes, when extracellular K^+ concentration is high and apical membrane potential is in the depolarized state.

The most striking functional abnormality in Kir4.1-deficient gastric mucosa was the enormously accelerated onset of acid secretion. Early studies suggested that the rate-limiting step in the onset of acid secretion is the fusion of tubulovesicles with the apical membrane (19–21). The conspicuous abnormality in the ultrastructure of the Kir4.1-deficient PCs was the fully elaborated secretory membrane with concomitant lack of tubulovesicular structures, despite the fact that the cells were functionally in a resting state (as evidenced by very low rates of acid secretion). These findings suggest that Kir4.1 channels may also be essential for the proper membrane recycling events during the recycling of membrane from the secretory canaliculi to the cytoplasmic tubulovesicular location and vice versa.

Comparing published ultrastructural abnormalities in other gene-deficient or transgenic mice with those in the Kir4.1$^{-/-}$ PC suggests that it may be the endocytotic recycling step from the secretory membrane that requires Kir channel activity. First, Nguyen *et al.* (22) described a mouse strain with a mutation in a tyrosine-based endocytosis motif in the H^+/K^+-ATPase β-subunit. The deletion of this motif prevents H^+/K^+-ATPase endocytosis and termination of acid secretion (23) and results in a PC morphology similar to the one seen in Kir4.1$^{-/-}$ mice. Fused secretory membranes with a lack of tubulovesicles are a hallmark of the altered ultrastructure of these PCs (22), similar to what we observed in Kir4.1$^{-/-}$ PCs. Second, Jain *et al.* (24) recently described the Hip1r-deficient mouse, which also displayed similar changes in PC ultrastructure compared with Kir4.1$^{-/-}$ mice, with fully elaborated secretory membranes in

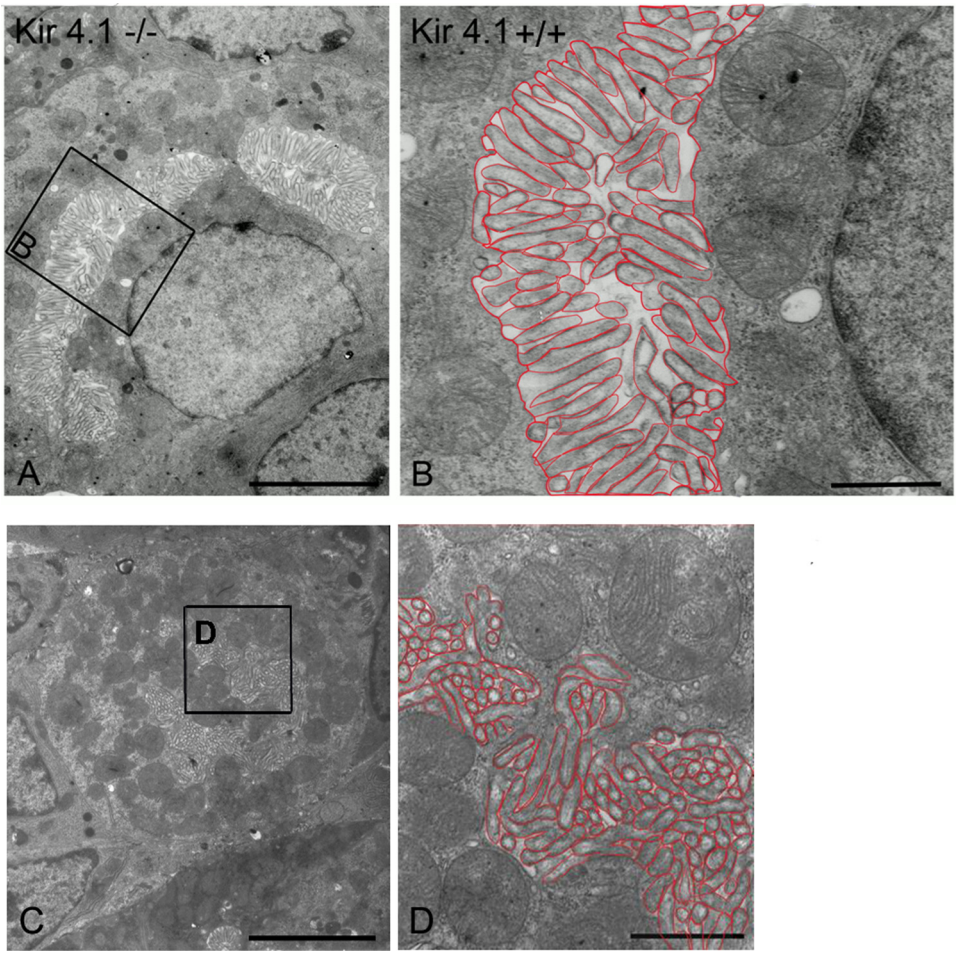

FIGURE 5. *A* and *C*, transmission electron microscopy of mucosa from unstimulated Kir4.1$^{-/-}$ oxyntic cells (low magnification survey of two PCs). The tight canaliculi are lined by numerous closely arranged microvilli. *B* and *D*, the framed region of a canaliculus is reproduced at higher magnification. The lining of the canaliculus by densely packed microvilli is evident. The adjacent cytoplasm on both sides of the canaliculus is devoid of tubulovesicles. The microvillar membrane is lined in *red*, and no typical tubulovesicles were found in Kir4.1$^{-/-}$ PCs. *Scale bars* = 5 μm (*A*, *C*) and 1 μm (*B*, *D*).

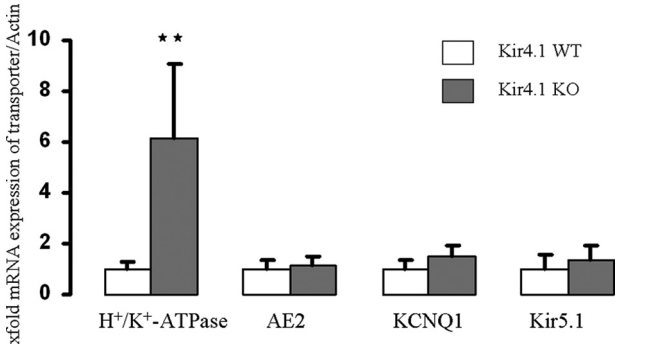

FIGURE 6. **mRNA expression of H$^+$/K$^+$-ATPase, AE2, KCNQ1, and Kir5.1 in Kir4.1$^{+/+}$ ($n = 4$) and Kir4.1$^{-/-}$ ($n = 4$) mice.** H$^+$/K$^+$-ATPase expression was significantly increased in Kir4.1$^{-/-}$ mice (**, $p < 0.01$), whereas the expression of AE2, KCNQ1, or Kir =5.1 was not significantly changed.

the absence of an acid secretory agonist and a lack of tubulovesicles. Interestingly, [^{14}C]aminopyrine accumulation as a measure of acid formation in isolated gastric glands was increased in the Hip1r mouse, whereas overall acid output into the lumina of the stomachs of anesthetized mice was decreased. The seemingly paradox situation may be explained by secondary changes in the gastric mucosa, with fundic hyperplasia and a strong increase in the mucous neck all zone, which can result in increased HCO_3^- secretion, as we have observed in adult KCNQ1-deficient mouse stomach (11). Hip1r is an F-actin- and clathrin-binding protein involved in vesicular trafficking (25, 26), and it was speculated that either the tubulovesicle insertion into or retrieval from the secretory membrane could be disturbed by lack of this protein.

There is also a mouse model with features of abundant tubulovesicles and lack of secretory membranes, the ezrin "knockdown" mouse (17). A large body of work exists demonstrating the importance of ezrin phosphorylation in stimulation-associated PC activation and transformation into the secretory state (1, 27–32). The ezrin knockdown mouse described by Tamura *et al.* (17) displayed a defect in the insertion of tubulovesicles into the apical membranes, with an accumulation of tubulovesicles in the cytoplasm and a scarcity of secretory membranes with short microvilli. The PC ultrastructure of the ezrin-deficient stomach is clearly completely different from that found in the Kir4.1$^{-/-}$ PC, arguing against the assumption that Kir4.1 deficiency may interfere with the insertion of tubulovesicles into the apical membrane.

Finally, the question remains if the tubulovesicles are absent because they are not formed at all in Kir4.1$^{-/-}$ PCs. Studying ultrastructural changes in Atp4α-deficient PCs, which lack the

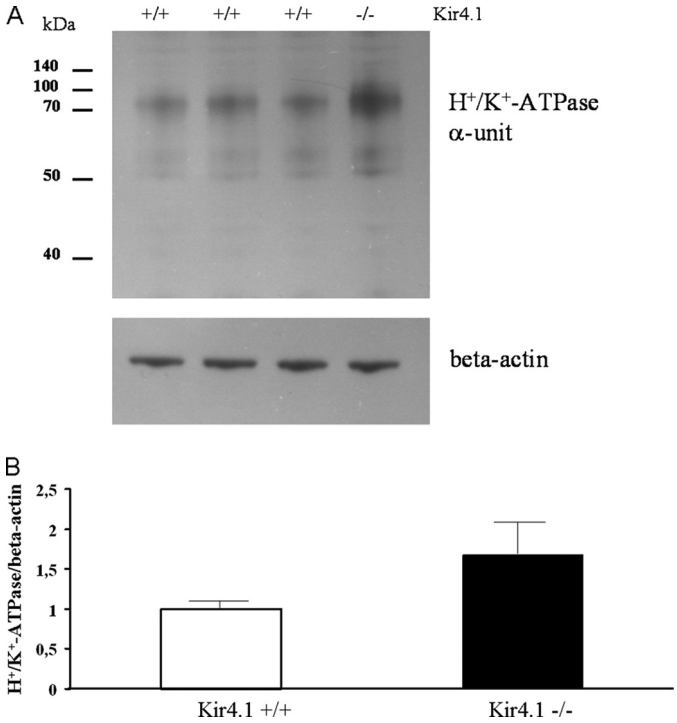

FIGURE 7. **H^+/K^+-ATPase α-unit protein expression is up-regulated in Kir4.1$^{-/-}$ mice.** *A*, Western blot for the gastric H^+/K^+-ATPase α-unit in mucosal homogenates from the three Kir4.1$^{+/+}$ mice and the one Kir4.1$^{-/-}$ mouse from one litter, showing a stronger band for the gastric H^+/K^+-ATPase α-unit in the Kir4.1$^{-/-}$ sibling. *B*, analysis of a total of four litters, containing one Kir4.1$^{-/-}$ offspring each, demonstrated a significant increase in relative gastric H^+/K^+-ATPase α-unit protein content in Kir4.1-deficient mucosa. $p < 0.05$.

H^+/K^+-ATPase α-unit, demonstrated a totally different situation from that in Kir4.1$^{-/-}$ PCs: instead of secretory membranes, large vacuoles with scant microvilli and very occasional vesicular structures resembling tubulovesicles are seen in Atp4α-deficient PCs (33). Clearly, the microvilli are long and well defined in Kir4.1$^{-/-}$ secretory membranes. Pettitt *et al.* (34) studied the ontogeny of the PC secretory membranes and tubulovesicles during embryonic development in mice and found that H^+/K^+-ATPase expression coincides with the formation of secretory membranes (rather than tubulovesicles) early in murine development and that tubulovesicles may form through endocytosis from the secretory membranes and are observed once the secretory membranes are well established. These findings also suggest that lack of tubulovesicles, but not of secretory membranes, may point to an endocytosis defect. We then asked the question whether the altered ultrastructure of Kir4.1$^{-/-}$ mice may reflect a general delay in PC development because of the growth deficit of these mice. Three observations argue against this. First, Kir4.1$^{-/-}$ mice were indistinguishable from WT mice until postnatal day 4, whereas Pettitt *et al.* (34) were able to see subapical tubulovesicles at embryo day 19. Second, when we reduced the litter size (genotyped very early after birth and removed the Kir4.1$^{+/-}$ mice), we had Kir4.1$^{-/-}$ survivors until days 12–14, and two of them were studied ultrastructurally. Although their body weight was larger compared with WT mice at day 7, the PC ultrastructure (elaborate secretory membranes and lack of tubulovesicles) looked similar to that of Kir4.1$^{-/-}$ between postnatal days 7–8 and 12, respectively, and very different from that of the WT between day 7 and Kir4.1$^{-/-}$ day 12. Third, we have studied the stomach of other transgenic mice that have growth deficits (NBCe1 KO and NKCC1 KO) in the suckling stage and have not observed this phenotype. Taken together, the ultrastructural abnormalities in Kir4.1$^{-/-}$ PCs clearly favor the notion of a recycling defect rather than a disturbance in the formation or fusion defect.

What may be the functional role of Kir4.1 channels in the control of acid secretion and the process of tubulovesicle endocytosis? Inwardly rectifying K^+ channels serve to restore membrane potential to K^+ equilibrium potential (35–37). Stimulation of acid secretion is associated with an initial PC hyperpolarization, presumably by KCNQ1 channel activation, followed by depolarization, presumably via the opening of Cl^- conductances (38–42). Kir channels would "shut down" under those circumstances, restoring polarization and preventing excess K^+ loss. Because extracellular K^+ *per se* is rate-limiting for acid secretion (in the presence of H^+/K^+-ATPase in the luminal membrane) (see Fig. 2), this function of the Kir channels may make physiological sense to curb the acid secretory rate, preserve cellular ATP, and stabilize the luminal membrane potential. If Kir channel ablation results in a shift of apical membrane potential to a more depolarized state, this could potentially favor KCNQ1 channel activity and result in excess K^+ secretion as well as proton pumping, explaining the observed gastric phenotype observed in our study. In favor of this hypothesis is the finding that an experimental increase in luminal K^+ concentration resulted in an increase in maximal acid secretory rates in WT mucosa, but not Kir4.1-deficient mucosa.

As our results indicate, Kir channels are not necessary for the PC to obtain maximal acid secretory rates. However, at the end of the acid secretory cycle, when K^+ concentration in the secretory canaliculi is high and the apical membrane is depolarized, the electrochemical gradient may even favor K^+ uptake via Kir channels. Because both high external K^+ and low pH prevent endocytosis in other cell types (5), the ionic environment in the secretory membrane at the end of the acid secretory cycle may interfere with tubulovesicle endocytosis unless regulated. In this scenario, Kir4.1 channels may be an essential factor in tubulovesicular recycling.

K^+ conductances have been implicated in the regulation of vesicle trafficking in other cell types at the level of the vesicle as well as the plasma membrane (44). In insulin-secreting cells, the closure of K_{ATP} channels by glucose-mediated ATP formation initiates the vesicle fusion event, and the activation of Kv2.1 channels terminates exocytosis (45). In addition, high extracellular K^+ was found to stimulate exocytosis in many systems (46), low pH inhibited endocytosis (5), and membrane potential was also found to influence PC tubulovesicular recycling in early studies (47, 48). Thus, it is not difficult to imagine that the presence of an inwardly rectifying K^+ channel coupled to an H^+/K^+-ATPase in the luminal membrane can be of great importance to the endocytotic process.

In summary, this study suggests that the physiological role of the PC Kir4.1 channels may be to provide a balance between rapid K^+ loss via KCNQ1 and K^+ absorption via the slower

action of the H^+/K^+-ATPase. Colocalized with the H^+/K^+-ATPase throughout the acid secretory cycle, Kir4.1 channels are likely to influence luminal K^+/H^+ concentration, membrane potential, and possibly other solute transporters in the secretory canaliculi. Their lack may result not only in an exaggerated acid secretory response but also in defects in intracanalicular volume control, and this may influence tubulovesicular membrane recycling. Kir4.1-deficient mice are, to our knowledge, the first mouse strain in which the deletion of a PC ion transporter results in an augmentation of acid secretory rate and may therefore serve to further understand the complex mechanism of H^+/K^+-ATPase trafficking and regulation. More work at a molecular level is needed to work out the details of this important regulatory role of PC Kir channels.

Acknowledgments—We thank Ulrike Dringenberg, Regina Engelhardt, Janina Bonhagen, and Brigitte Rausch for breeding and genotyping of mice and technical expertise and Georg Sachs, Shmuel Muallem, Jens Leipziger, and Markus Bleich for helpful discussions and manuscript critique.

REFERENCES

1. Schubert, M. L. (2009) *Curr. Opin. Gastroenterol.* **25,** 529–536
2. Yao, X., and Forte, J. G. (2003) *Annu. Rev. Physiol.* **65,** 103–131
3. Cuppoletti, J., and Sachs, G. (1984) *J. Biol. Chem.* **259,** 14952–14959
4. Forte, J. G., and Zhu, L. (2010) *Annu. Rev. Physiol.* **72,** 273–296
5. Smith, R. M., Baibakov, B., Lambert, N. A., and Vogel, S. S. (2002) *Traffic* **3,** 397–406
6. Forte, J. G. (2004) *Am. J. Physiol. Cell Physiol.* **286,** C478–C479
7. Heitzmann, D., and Warth, R. (2008) *Physiol. Rev.* **88,** 1119–1182
8. Dedek, K., and Waldegger, S. (2001) *Pflugers Arch.* **442,** 896–902
9. Lambrecht, N. W., Yakubov, I., Scott, D., and Sachs, G. (2005) *Physiol. Genomics* **21,** 81–91
10. Roepke, T. K., Anantharam, A., Kirchhoff, P., Busque, S. M., Young, J. B., Geibel, J. P., Lerner, D. J., and Abbott, G. W. (2006) *J. Biol. Chem.* **281,** 23740–23747
11. Song, P., Groos, S., Riederer, B., Feng, Z., Krabbenhöft, A., Smolka, A., and Seidler, U. (2009) *J. Physiol.* **587,** 3955–3965
12. Fujita, A., Horio, Y., Higashi, K., Mouri, T., Hata, F., Takeguchi, N., and Kurachi, Y. (2002) *J. Physiol.* **540,** 85–92
13. Malinowska, D. H., Sherry, A. M., Tewari, K. P., and Cuppoletti, J. (2004) *Am. J. Physiol. Cell Physiol.* **286,** C495–C506
14. Kaufhold, M. A., Krabbenhöft, A., Song, P., Engelhardt, R., Riederer, B., Fährmann, M., Klöcker, N., Beil, W., Manns, M., Hagen, S. J., and Seidler, U. (2008) *Gastroenterology* **134,** 1058–1069
15. Kofuji, P., Ceelen, P., Zahs, K. R., Surbeck, L. W., Lester, H. A., and Newman, E. A. (2000) *J. Neurosci.* **20,** 5733–5740
16. Deleted in proof
17. Tamura, A., Kikuchi, S., Hata, M., Katsuno, T., Matsui, T., Hayashi, H., Suzuki, Y., Noda, T., Tsukita, S., and Tsukita, S. (2005) *J. Cell Biol.* **169,** 21–28
18. Neusch, C., Rozengurt, N., Jacobs, R. E., Lester, H. A., and Kofuji, P. (2001) *J. Neurosci.* **21,** 5429–5438
19. Forte, T. M., Machen, T. E., and Forte, J. G. (1977) *Gastroenterology* **73,** 941–955
20. Clausen, C., Machen, T. E., and Diamond, J. M. (1983) *Biophys. J.* **41,** 167–178
21. Clausen, C., Machen, T. E., and Diamond, J. M. (1982) *Science* **217,** 448–450
22. Nguyen, N. V., Gleeson, P. A., Courtois-Coutry, N., Caplan, M. J., and Van Driel, I. R. (2004) *Gastroenterology* **127,** 145–154
23. Courtois-Coutry, N., Roush, D., Rajendran, V., McCarthy, J. B., Geibel, J., Kashgarian, M., and Caplan, M. J. (1997) *Cell* **90,** 501–510
24. Jain, R. N., Al-Menhali, A. A., Keeley, T. M., Ren, J., El-Zaatari, M., Chen, X., Merchant, J. L., Ross, T. S., Chew, C. S., and Samuelson, L. C. (2008) *J. Clin. Invest.* **118,** 2459–2470
25. Engqvist-Goldstein, A. E., Warren, R. A., Kessels, M. M., Keen, J. H., Heuser, J., and Drubin, D. G. (2001) *J. Cell Biol.* **154,** 1209–1223
26. Schafer, D. A. (2002) *Curr. Opin. Cell Biol.* **14,** 76–81
27. Pagliocca, A., Hegyi, P., Venglovecz, V., Rackstraw, S. A., Khan, Z., Burdyga, G., Wang, T. C., Dimaline, R., Varro, A., and Dockray, G. J. (2008) *Exp. Physiol.* **93,** 1174–1189
28. Zhou, R., Zhu, L., Kodani, A., Hauser, P., Yao, X., and Forte, J. G. (2005) *J. Cell Sci.* **118,** 4381–4391
29. Zhou, R., Cao, X., Watson, C., Miao, Y., Guo, Z., Forte, J. G., and Yao, X. (2003) *J. Biol. Chem.* **278,** 35651–35659
30. Agnew, B. J., Duman, J. G., Watson, C. L., Coling, D. E., and Forte, J. G. (1999) *J. Cell Sci.* **112,** 2639–2646
31. Hanzel, D., Reggio, H., Bretscher, A., Forte, J. G., and Mangeat, P. (1991) *EMBO J.* **10,** 2363–2373
32. Mangeat, P., Gusdinar, T., Sahuquet, A., Hanzel, D. K., Forte, J. G., and Magous, R. (1990) *Biol. Cell* **69,** 223–231
33. Spicer, Z., Miller, M. L., Andringa, A., Riddle, T. M., Duffy, J. J., Doetschman, T., and Shull, G. E. (2000) *J. Biol. Chem.* **275,** 21555–21565
34. Pettitt, J. M., Toh, B. H., Callaghan, J. M., Gleeson, P. A., and Van Driel, I. R. (1993) *Immunol. Cell Biol.* **71,** 191–200
35. Reimann, F., and Ashcroft, F. M. (1999) *Curr. Opin. Cell Biol.* **11,** 503–508
36. Olsen, M. L., and Sontheimer, H. (2008) *J. Neurochem.* **107,** 589–601
37. Neusch, C., Weishaupt, J. H., and Bähr, M. (2003) *Cell Tissue Res.* **311,** 131–138
38. Debellis, L., Curci, S., and Frömter, E. (1992) *Pflugers Arch.* **422,** 253–259
39. Debellis, L., Curci, S., and Frömter, E. (1990) *Am. J. Physiol.* **258,** G631–G636
40. Ueda, S., and Okada, Y. (1989) *Biochim. Biophys. Acta* **1012,** 254–260
41. Ueda, S., Loo, D. D., and Sachs, G. (1987) *J. Membr. Biol.* **97,** 31–41
42. Tsunoda, Y., and Matsumiya, H. (1987) *FEBS Lett.* **222,** 149–153
43. McDaniel, N., Pace, A. J., Spiegel, S., Engelhardt, R., Koller, B. H., Seidler, U., and Lytle, C. (2005) *Am. J. Physiol. Gastrointest. Liver Physiol.* **289,** G550–G560
44. Thévenod, F. (2002) *Am. J. Physiol. Cell Physiol* **283,** C651–C672
45. Hou, J. C., Min, L., and Pessin, J. E. (2009) *Vitam. Horm.* **80,** 473–506
46. Raiteri, L., Zappettini, S., Milanese, M., Fedele, E., Raiteri, M., and Bonanno, G. (2007) *J. Neurochem.* **103,** 952–961
47. Ostrowski, J., Jarosz, D., Zych, W., and Wojciechowski, K. (1994) *J. Physiol. Pharmacol.* **45,** 351–360
48. Ostrowski, J., Dołowy, K., Zych, W., and Butruk, E. (1991) *J. Physiol. Pharmacol.* **42,** 367–379